

## Chapter 2

# Synthesis of High-Nitrogen Energetic Material

Mikhail I. Eremets, Ivan A. Trojan, Alexander G. Gavriliuk,  
and Sergey A. Medvedev

### 2.1 Introduction

Pure nitrogen can be considered as a material with optimized storage of chemical energy because of the huge difference in energy between triply bonded di-nitrogen and singly bonded nitrogen.  $\text{N} \equiv \text{N}$  bond is one of the strongest chemical bonds known, containing  $4.94 \text{ eV atom}^{-1}$  while the  $\text{N}-\text{N}$  bond is much weaker with  $-0.83 \text{ eV atom}^{-1}$  [1]. Therefore when transforming from singly bonded nitrogen to diatomic triply bonded molecular nitrogen, a large amount of energy should be released: about  $2.3 \text{ eV atom}^{-1}$ . Or, in other words, this chemical energy can be ideally stored by transforming a triple bond into three single bonds. Thus, nitrogen may form a high-energy density material with energy content higher than that of any known nonnuclear material. The greatest utility of fully single-bonded nitrogen would be as high explosives. Here, a tenfold improvement in detonation pressure over HMX (one the more powerful high explosives) seems possible [2].

A chemical approach for synthesis of nitrogen-energetic materials is creating large all-nitrogen molecules or clusters bound by single ( $\text{N}-\text{N}$ ) or single and double ( $\text{N}=\text{N}$ ) bonds. Calculations predict different polynitrogen molecules or clusters [3] such as, for instance,  $\text{N}_4$ ,  $\text{N}_8$ ,  $\text{N}_{20}$ , or even nitrogen fullerene  $\text{N}_{60}$  (see for review Refs [3–5]) with high-energy-storage capacity. However, none of them has yet been synthesized with exception of  $\text{N}_4(\text{TdN}_4)$  [6], albeit with a very short lifetime of  $\sim 1 \mu\text{s}$  [6]. Synthesis of compounds having several nitrogen atoms consecutively is difficult because the single bond in nitrogen is relatively weak. It has been achieved only in compounds with other atoms. For instance,  $\text{HN}_3$  and other azides with linear- $\text{N}_3$  radical have been synthesized by Curtius in 1890 [7]. Only recently  $\text{N}_5^+$  was synthesized by Christe and coworkers [8]. On the basis of the  $\text{N}_3^-$  and  $\text{N}_5^+$  species nearly all nitrogen compounds were synthesized by attaching these radicals to a central atom of Te, B, and P such as  $\text{N}_5\text{P}(\text{N}_3)_6$ ,  $\text{N}_5\text{B}(\text{N}_3)_4$ ,  $\text{Te}(\text{N}_3)_4$ , and others (see for review Refs [2, 9–11]).

Presented here is an ultimate case of pure single-bonded nitrogen which can be synthesized at high pressures and temperatures from common triply bonded molecular nitrogen. At high pressures molecules of nitrogen approach each other and start interacting so strongly that intramolecular interaction becomes comparable with intermolecular interaction, and therefore di-nitrogen molecules can dissociate to atomic nitrogen. Atoms of nitrogen with three directed covalent bonds can further create a three-dimensional network popularly termed polymeric nitrogen. Such transformations have been predicted long time ago [12, 13] to happen at high pressures of  $\approx 50$  GPa, but it was found experimentally at much high pressures of  $\sim 200$  GPa [14] at low temperatures, and then at a slightly lower pressures of 150 GPa and room temperature [15]. This apparently nonmolecular nitrogen has a disordered network of single- and double-bonded atoms as follows from calculations [16, 17].

Next important step in the preparation of polymeric nitrogen was the theoretical prediction of single-bonded crystalline nitrogen where each nitrogen atom is connected with three other with single bonds [18]. It has a cubic symmetry structure but with an unusual arrangement of atoms: the cubic gauche structure (referred to as cg-N or CG) of the  $I2_13$  space group. This structure was recently fully confirmed experimentally [19–22]. Theoretical calculations also agree that the cg-N structure is the most stable among possible proposed single-bonded nitrogen networks [23–29]. This polymeric nitrogen is a unique material. First of all, it has very high accumulated energy: about  $1.2\text{--}1.5\text{ eV atom}^{-1}$  releases during the transformation from cg-N to  $\text{N}_2$  [16–18, 30]. This is 5.5 times higher (energy/mass ratio) when compared to the powerful explosive hexogen [17]. At the same time cg-N is similar to diamond in terms of values of lattice parameters and low compressibility. Thus it could be a hard (or superhard) material with ultimate high-energy capacitance. Importantly, polymeric nitrogen is predicted to be metastable at ambient pressure [18], and an amorphous polymeric nitrogen indeed has been recovered to ambient pressure at low temperatures [14]. Cg-N was proved experimentally to be metastable at least down to 25 GPa. This chapter describes the synthesis and properties of polymeric nitrogen in more detail, and also discusses other polymeric structures which are predicted to be competitive with the cg-N phase in some pressure range [23, 25–28, 31–33].

Finally we mention attempts to decrease the pressure of polymerization by using precursors different from pure nitrogen. Instead of compressing diatomic nitrogen, molecular  $\text{N}_3^-$  anions in the lattice of  $\text{NaN}_3$  were examined [34, 35]. The  $\text{N}_3^-$  anion is a straight chain of three nitrogen atoms linked essentially with double bonds. It can be considered as a molecule which is more weakly bonded than the diatomic triple-bonded nitrogen. Therefore, it could be expected that the  $\text{N}_3^-$  molecules will create polymeric single-covalent bond networks easier than diatomic nitrogen. New structures that are distinct from linear  $\text{N}_3^-$ -ion-based molecular phases were found near ambient pressure after laser heating [34]. In Ref. [35] the photolytic decomposition of sodium azide under UV pulse irradiation was studied. The resultant product, speculated to be  $\text{N}_7^-$ , was found to be unstable at room pressure and temperature.

## 2.2 Polymeric Nitrogen

In this section we will present our results on synthesis and properties of polymeric single-bonded nitrogen. When nitrogen atoms are connected with *single bonds* into a polymeric network it could be a high-energy density material (HEDM). Moreover, polymeric nitrogen should be environmentally clean because the final product of the transformation is nitrogen. This polymeric nitrogen material could also be an ideal rocket fuel or propellant.

A way to create an atomic solid with a single-bonded crystalline structure is application of high pressures, as predicted in 1985 by McMahon and LeSar [12]. Simple cubic or distorted sc structures similar to other group-V elements were calculated. This transformation is expected to accompany with a large drop of volume and considerable hysteresis. This new material can be called “polymeric nitrogen”: the starting dimer is the molecular nitrogen while the final product is a crystal built with single covalent bonds. We note here that nitrogen behaves uniquely under pressure. If we compare it with other molecular solids such as  $\text{H}_2$ ,  $\text{O}_2$ ,  $\text{I}_2$ , and others [36], they are double-covalent bonded and at high pressure transform to metals while nitrogen first transforms to an insulating covalent crystal. Nitrogen also is different from other elements of group V. For instance, the stable form of phosphorus at ambient pressure is a  $\text{P}_4$  molecule where atoms are connected to each other by single bonds. The reason of this difference is simple: atoms of phosphorous are significantly larger than nitrogen atoms and therefore longer single bonds are preferable. At high pressure nitrogen also does not follow the sequence of phase transformations typical for group-V elements.

Mailhot et al. [18] found that nitrogen behaves uniquely under pressure: molecular nitrogen transforms into a lattice of single-bonded atoms with cubic gauche structure (cg-N). This unusual structure naturally follows from the directed covalent bonds: the dihedral angle in a N–N single bond energetically prefers a *gauche* conformation [18] as can be seen, for instance, in the molecule of hydrazine. As a result this structure theoretically is much more preferable (Fig. 2.1): it has significantly lower ( $0.86 \text{ eV atom}^{-1}$ ) total energy than previously considered phases. This has been confirmed in numerous calculations [17, 23–28, 30, 32, 37–44].

Mailhot et al. [18] calculated the volume, bulk modulus, and other properties of cg-N. This transformation should happen at  $\approx 50 \text{ GPa}$  and be accompanied with a dramatic drop of volume ( $\sim 20\%$ ) and complete change of the phonon spectrum. The cg-N phase was predicted to be metastable at ambient pressure. All this gave clear information for experimental proof. However, the experiments that followed did not reveal any transition in this pressure range while a darkening [45] and nearly opaque state [46] has been observed at the highest pressures up to  $180 \text{ GPa}$  [46].

Transformation to nonmolecular nitrogen finally came with the dramatic disappearance of the molecular vibron [14] at  $190 \text{ GPa}$  at low temperatures from transparent to an opaque phase. The same transition was also seen in measurements at room and elevated temperatures [15, 47, 48]. It was found that this transformation has a huge hysteresis [14]. Therefore, the value of equilibrium pressure is about  $100 \text{ GPa}$  [14] – much lower than the pressure of direct transformation, and closer

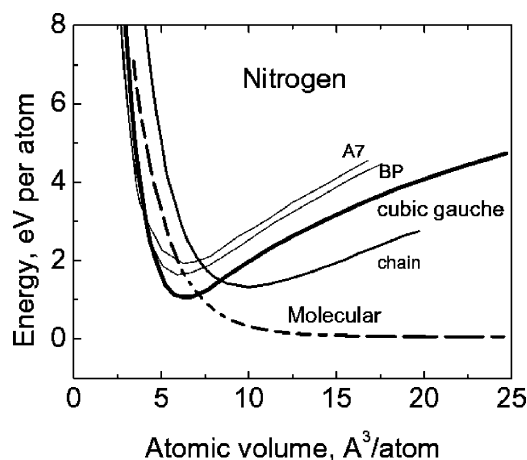


**Fig. 2.1** Polymeric phases of nitrogen. Total energy per atom calculated for the threefold-coordinated arsenic (A7), black-phosphorus (BP), and cubic gauche (cg) phases of nitrogen, and for a twofold-coordinated chainlike (ch) phase of nitrogen, as a function of atomic volume (after Mailhot et al. [18])

to the theoretical [18] calculations. Moreover, the hysteresis was so large that it allowed the nonmolecular nitrogen to be recovered at low temperatures [14]. Though the nonmolecular nitrogen has properties close to those predicted for the polymeric nitrogen [18], the material was a narrow-gap semiconductor [14, 16, 47], which is in contradiction to the predicted dielectric cg-N. First-principle simulations elucidated the structure of the opaque phase: an amorphous or disordered network of single- and double-bonded nitrogen atoms [16, 17] as shown in Fig. 2.2a. However, there is no direct experimental evidence that the nonmolecular phase creates a polymeric network. Available optical data only indicate the amorphous nature for this material [14, 16, 47]. This can be seen, for instance, from Fig. 2.2b where only very broad bands are present in the Raman spectrum.

Next decisive step towards polymeric nitrogen was done with laser heating of molecular nitrogen above 100 GPa [19]. Here a direct transformation of molecular nitrogen to a new transparent phase, which turned out to be the long sought after polymeric nitrogen was found. Polymeric nitrogen was synthesized at  $T > 2,000\text{ K}$  at  $P > 110\text{ GPa}$ . These record parameters were achieved from a novel arrangement of the diamond anvil cell (Fig. 2.3). First, a gasket compacted from powdered cubic boron nitride (cBN) mixed with epoxy was used [49]. This gasket is 1.5–2 times thicker (8–10  $\mu\text{m}$  at 60 GPa) than typical hard gasket materials such as Re or W at the same pressure. This allows larger sample volumes. Also, this increases the gap between the boron laser radiation absorber (that heats the sample) and the anvils (Fig. 2.3), a precondition to achieving very high temperatures at megabar pressures. Second, the cell was specifically designed for use in with challenging x-ray diffraction measurements. X-ray diffraction measurements of a nitrogen sample (which is a light element and a weak scatterer) at pressures up to 170 GPa were performed

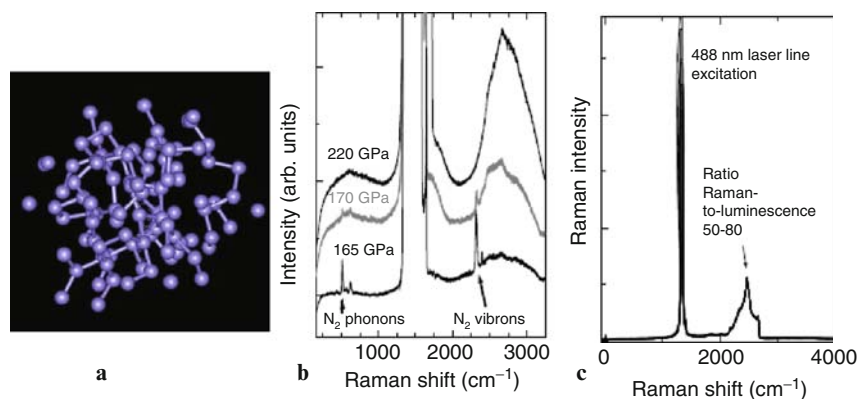


**Fig. 2.2** Amorphous polymeric nitrogen. (a) Structure of low-coordinated ( $Z = 3-4$ ) nitrogen at ambient pressure at 100 K produced by simulations showing atom positions and bonds between them (from Ref. [16]). (b) Raman spectra of nitrogen at megabar pressures at 300 K taken through diamond anvils having a negligible own luminescence as can be seen from (c) where Raman spectra from 15 anvils are presented which perfectly coincide: only first- and second-order Raman peaks from diamond are in the spectra

at the ID9 beam line at ESRF [50]. The cBN gasket is extremely advantageous in x-ray diffraction studies: it produces only a few weak peaks comparable with nitrogen in intensity. Also, boron as an absorber of the  $1.064\ \mu\text{m}$  laser radiation was used (Fig. 2.3a). Importantly, boron is a very weak scatterer of x-rays and a signal produced by a  $1\ \mu\text{m}$  thick plate does not interfere with the diffraction pattern from the nitrogen sample. Moreover, the weak diffraction peaks from boron are uniformly distributed over a wide spectrum without strong peaks [51]. The boron plate was formed by pressing nanoparticles of amorphous boron of 99.99% purity. Boron is initially a semiconductor and transforms to a poor metal at megabar pressures [49]. It is a good absorber of the  $1.06\ \text{mm}$  laser radiation, however it violently reacts with nitrogen at  $T > 1,800\ \text{K}$  and pressures  $< 15\ \text{GPa}$  [52]. At megabar pressures this reaction is nearly suppressed. We observed small color changes at the center of the boron plate at the highest temperatures that are likely due to formation of cBN, as evident from well-recognized peaks of cBN in the diffraction pattern (Fig. 2.3). However, the thin boron/cBN plate remained opaque, and heating was very stable to the highest temperatures allowing reliable temperature measurements [53]. Note, that at pressure below  $\sim 50\ \text{GPa}$  reaction of boron with nitrogen becomes marked.

Heating to high temperature released stress inside the sample, resulted in sharp x-ray diffraction peaks (Fig. 2.3), and dramatically increased the accuracy of the measurements. For pressure measurements ruby luminescence was used [54]. For that a micrometer-sized piece of ruby was placed at the edge of the gasket hole. To study the possible reaction of ruby with nitrogen, ruby was omitted in another experiment, yielding the same result. The pressure in this experiment was determined from the sharp high-frequency edge of the diamond anvil [55]. The diamond anvil cell of original construction was described elsewhere [56]. Nitrogen gas compressed to 2,500 bars was loaded at room temperature. Very low-luminescence synthetic

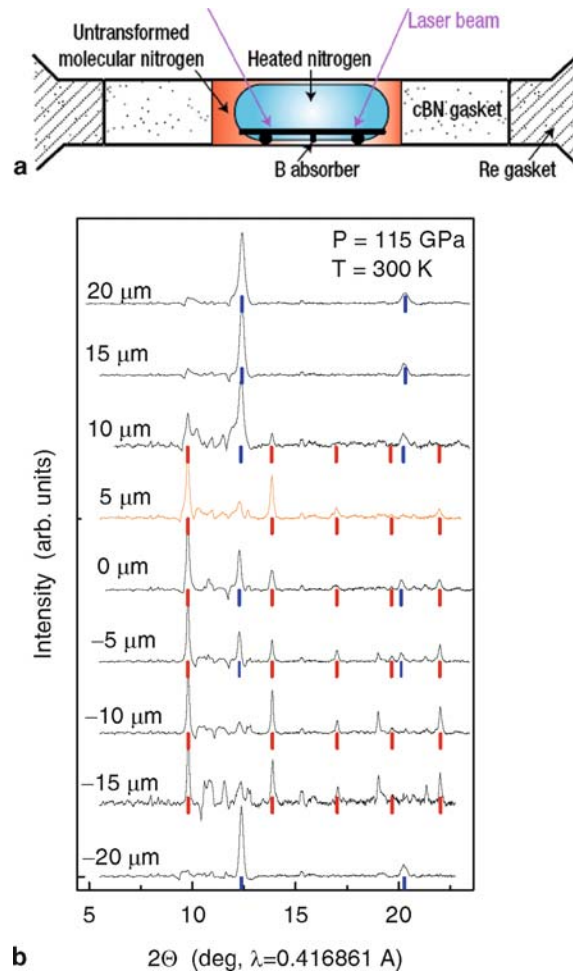


**Fig. 2.3** X-ray diffraction measurements of nitrogen after heating to 2,600 K at 140 GPa. (a) A cross section of the sample arrangement. The heating  $\sim 1\text{ }\mu\text{m}$ -thick boron plate (absorber of laser radiation; black) rests on cBN pieces that thermally insulate the plate from the bottom anvil. The sample squeezed between the anvils is surrounded by the cBN/epoxy gasket followed by the metallic (Re) supporting ring. The culet of diamond anvil is of diameter  $90\text{ }\mu\text{m}$ . X-ray diffraction was measured with a monochromatic X-ray beam with  $0.4168\text{ }\text{\AA}$  wavelength focused to a spot of diameter  $\sim 5\text{ }\mu\text{m}$ . (b) X-ray patterns taken across the culet of diamond anvil to distinguish between the input from the gasket and the different phases of the sample. Spectra taken from the most heated part ( $\pm 5\text{ }\mu\text{m}$ ) were attributed to the new phase of nitrogen. At the gasket only pure cBN patterns are present. At the edge of the nitrogen sample ( $r = -15\text{ }\mu\text{m}$ ) there is a significant input from the molecular phase at the  $10^\circ\text{--}14^\circ$  range. The black and grey vertical lines indicated calculated positions of reflections corresponding to cg-N and cBN, respectively

diamonds (Fig. 2.2) with flats of diameter  $95\text{ }\mu\text{m}$  beveled at  $10^\circ$  to  $380\text{ }\mu\text{m}$  culet and  $60\text{--}90\text{ }\mu\text{m}$  flats were used in other runs. Raman spectra before and after heating

were recorded with a single grating monochromator, notch-filters, cooled CCD and argon and Ti-sapphire lasers at the 458–800 nm spectral range.

In a typical run, the pressure was increased up to 140 GPa at 300 K until the sample started to darken. At this pressure, the sample was heated in steps with intermediate recordings of Raman spectra at room temperature. After the first heating to 980 K, the transformation accelerated. The sample darkened further, but it remained in the molecular state – the vibrons in the Raman spectra of nitrogen did not change. The high-frequency edge from the diamond anvils sharpened, indicating uniform pressure distribution, which dropped to 120 GPa. No further changes were observed after heating up to 1,400 K. After heating to 1,700 K, the sample further darkened and the intensity of the vibron of nitrogen significantly decreased.

At 1,980 K, the vibron peaks became indistinguishable from the background, all wide bands in the low-frequency part of spectrum disappeared, and luminescence measured from the nitrogen sample significantly increased. A ring around the absorber appeared, likely due to melting of the sample. Instead of further darkening, unexpectedly, the sample became transparent (the absorber plate became clearly visible in reflected light). After successive heating up to 2,500 and 2,600 K, the transparent colorless part spread out over a larger area and could be seen in transmitted light. The nitrogen at the edge of the gasket hole was not heated to the high temperatures and remained dark. The pressure in the center of the sample reduced to 115 GPa.

Thus, a dramatic transition happened at 115 GPa at temperatures above  $\sim 2,000$  K. X-ray diffraction patterns were accumulated from different parts of the sample across the culet in order to distinguish between the contribution from the gasket and the different phases of the sample (Fig. 2.3). In the center of the sample there are up to five reflections of the new phase of nitrogen and two reflections from cBN. These reflections are clearly different: the nitrogen rings are spotty while the cBN ring is not. In addition, the intensity of the cBN peaks varies from point to point of the scan, and at some places the reflections almost disappear.

We fitted the measured x-ray diffraction spectra by the cubic gauche structure of nitrogen (cg-N) and cBN. cg-N has the following parameters: space group  $I2_13$ ,  $a_0 = 3.4542 \text{ \AA}$ , sites  $8a$ ,  $x = 0.067$ . We tried also to fit the spectra to different proposed polymeric structures [12,13,17,25,37] as well as boron from the absorber [51] instead of the cg-N structure, but without satisfactory results. The cg-N structure is schematically shown in Fig. 2.4. All nitrogen atoms are threefold coordinated and bond-lengths are the same for all pairs of bonded atoms. At a pressure of 115 GPa the bond length is  $1.346 \text{ \AA}$  and the angle between bonds is  $108.87^\circ$ . We also determined the cg-N structure upon decreasing pressure down to 42 GPa (Fig. 2.4c). We fitted the experimental points measured in the 42–134 GPa range with Birch-Murnaghan equation of states (EOS) extrapolated to zero pressure with the following parameters: bulk modulus  $B_0 = 298 \text{ GPa}$ ,  $B' = 4.0$ ,  $V_0 = 6.592 \text{ \AA}^3$  [3]. The cg-N is a stiff solid as follows from the high value of  $B_0$  which is characteristic for strong covalent solids ( $B_0 = 365 \text{ GPa}$  for cBN [57]). The bulk modulus determined from different types of EOSs lies in the range of 300–340 GPa. The determined value of atomic volume  $V_0$  is close to  $6.67 \text{ \AA}^3$  [3] predicted in Ref. [18].



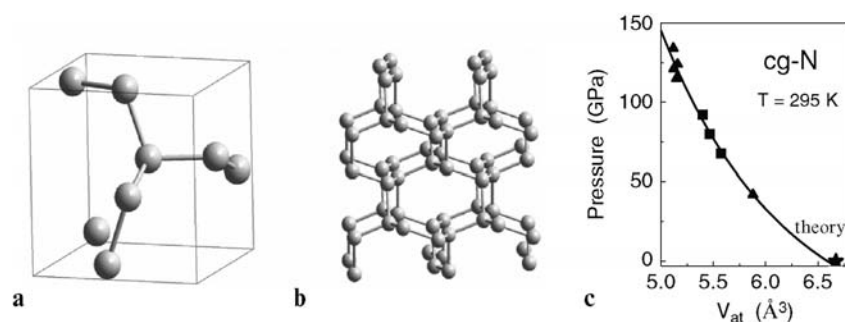


**Fig. 2.4** Cubic gauche (cg-N) structure. Each atom of nitrogen is connected to three neighbors with three single covalent bonds. **(a)** The primitive cell, **(b)** an extended structure of the polymeric nitrogen. **(c)** The EOS of cg-N structure. Extrapolation of this EOS to zero pressure gives a volume of cg-N structure about  $6.6 \text{ \AA}^3$  [3] – in excellent agreement with theoretical predictions of  $6.67 \text{ \AA}^3$  [3] (Ref. [18])

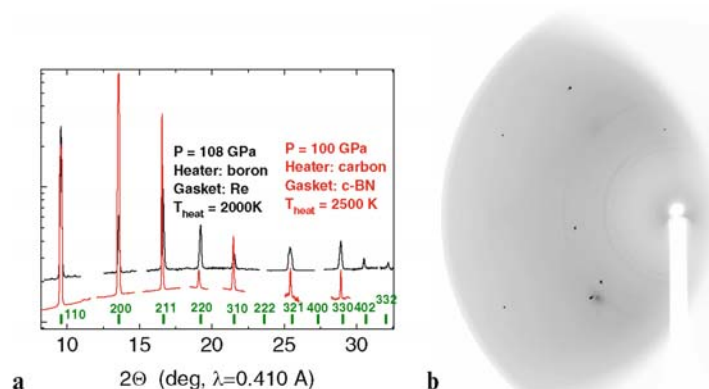


**Fig. 2.5** Diffraction from cg-N synthesized at 110 GPa in diamond anvil cell with laser heating. **(a)** Diffraction peaks from two experiments. Grey lines relates to the arrangement with boron absorber heated to 2,000 K and rhenium gasket. Black lines: CVD diamond plate heated to 2,500 K, gasket was prepared from cBN powder mixed with small amount epoxy. Numbers and rods are indexes and position of reflections calculated according to the cubic gauche structure. The peaks are obtained by integration of spots at diffraction pattern shown in **(b)** for the case of a cell with side-input for x-ray beam and combination of boron heater and Re gasket

The cg-N structure has been further confirmed in many experiments [20–22]. For instance, more x-ray reflections were obtained to check cg-N structure [58]. For that a diamond anvil cell, which allows collection of diffraction at higher angles has been built. It has an additional side-input at  $15^\circ$  to the axes of the cell. If the x-ray goes through this window the diffraction rays can be observed up to  $35^\circ$ . An example of the x-ray diffraction for this side-input geometry is shown in Fig. 2.5. Thus two new 321 and 330 reflections of cg-N structure were found. In other experiments with this geometry but with different arrangement of the gasket and the heater 402



and 332 reflections in addition were obtained. Altogether nine reflections from the sample were collected. These reflections were observed also because instead of a fine powder of cg-N larger crystallites were grown which can give strong reflections at large angles. For that, the synthesis temperature was kept as low as possible at a given pressure, and the heating time was increased to minutes. Thus conditions of equilibrium growth were approached.

An absorber of the laser radiation gives an additional complication for analysis and interpretation of the experiment. Therefore, cg-N also has been attempted to synthesize with laser heating but without any absorber. Nitrogen at pressures above  $\sim 130$  GPa significantly absorbs itself and it was successfully heated directly with YAG laser radiation resulting x-ray diffraction and Raman spectra of cg-N [20–22].

To summarize, we found the cg-structure which was considered theoretically as the most energetically favorable single-bonded structure [17, 23–28, 30, 32, 37–44] and originally proposed by Mailhot et al. [18]. This is a new allotrope of nitrogen where all atoms are connected with single covalent bonds. To our knowledge, this unusual cubic phase has not been observed previously in any element.

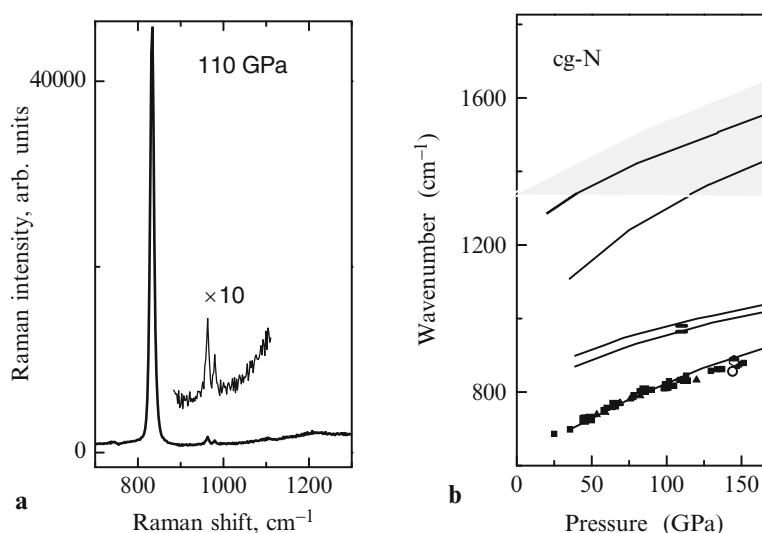


**Fig. 2.6** Raman scattering from the cubic gauche polymeric nitrogen. **(a)** Raman spectrum from a large sample of cg-N at 120 GPa. A small intensity doublet at  $963\text{ cm}^{-1}$  has been magnified for clarity. **(b)** Pressure dependence of Raman modes of the cg-N phase. Points are taken from different experiments. Lines are theoretical calculations [24]. The shadow area indicates width of Raman band from the stressed diamond anvils which covers the high-energy Raman lines of cg-N

### 2.2.1 Raman Spectra of *cg-N*

Transformation to *cg-N* phase was accompanied with a dramatic change of vibration spectra: after disappearing of the molecular vibron a new Raman peak in the *cg-N* phase was observed (Fig. 2.6). This is a fingerprint of transformation. The new peak is easily detected and it is strong in some samples. The position of this peak and its pressure dependence well follows calculations for *cg-N* phase [39] (Fig. 2.6). However, puzzlingly only one peak was observed in all experiments while four peaks are expected from the symmetry  $I2_13$  of *cg*-structure. Only recently this problem has been resolved. From theoretical side, intensities of Raman peaks along with their positions have been calculated in Ref. [24] and it was found that only one peak dominates, others should be much weaker. Experimentally this was confirmed by obtaining a strong Raman signal from a large sample. It was grown in a diamond cell with anvil culets of the toroidal shape [22] (Fig. 2.7). This shape dramatically

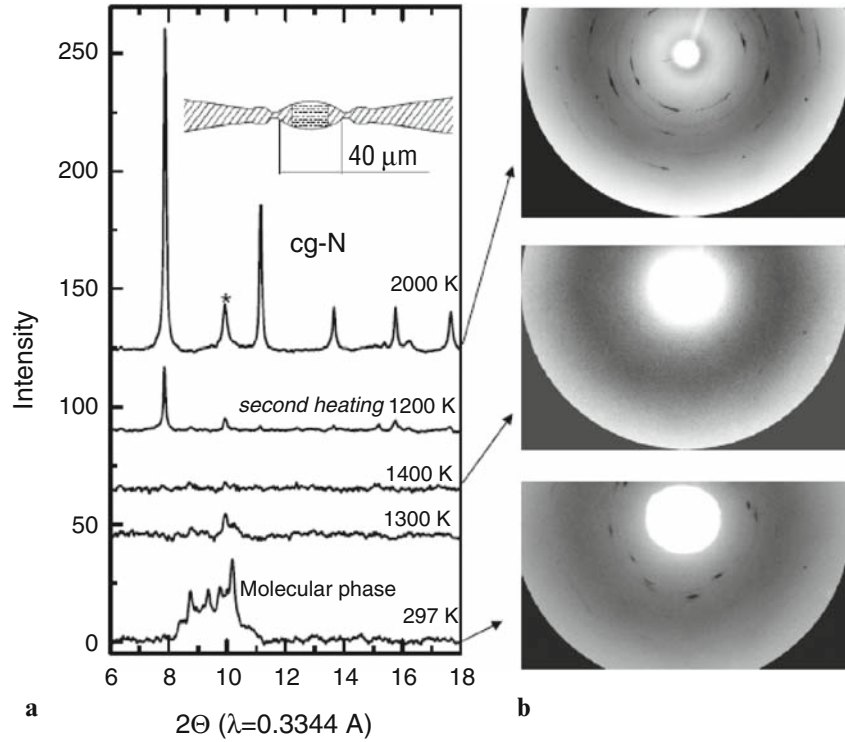


**Fig. 2.7** X-ray diffraction measurements of nitrogen at 140 GPa measured in situ at different temperatures. (a) The X-ray Diffraction spectra were obtained by integrating the CCD image patterns (shown at (b)) and extracting the background. Star indicates the cBN peak. X-ray beam with 0.3344 Å wavelength was focused to a spot of diameter  $\approx 5 \mu\text{m}$  and collimated by a  $20 \mu\text{m}$  pinhole. The radiation from the YAG laser was focused in the same place. Toroidal profile of diamond anvil culets is shown in inset (a)

increases the high-pressure volume and allows large samples to be obtained and consequently to have intensive x-ray diffraction (Fig. 2.7) and Raman spectra (Fig. 2.6). Thus we were able to analyze the Raman spectrum of cg-N in detail and to find one more additional weak split peak (Fig. 2.6). Its position as well as the intensities (which are  $\sim 100$  times smaller than that of the dominated Raman peak) coincides well with the calculations [24, 39]. The remaining two weak peaks owing to cg-N structure [24, 39] can be hidden under the strong background of the Raman band from the stressed diamond anvils (the dashed area at Fig. 2.6).

### 2.2.2 Control Experiments

In the experiments performed at high temperatures  $T > 2,000$  K, reaction of hot nitrogen with heater or surrounding gasket or diamonds is not excluded. Therefore, we had done numerous checking experiments to insure that the observed Raman and x-ray diffraction signals belong to cg-N, not to a product of interaction of nitrogen with gasket, absorber, or diamond. Different combinations of absorber and gasket materials (boron–cBN, boron–rhenium, -TiN–rhenium, beryllium–cBN, hBN–rhenium) results in the same x-ray diffraction pattern and Raman spectrum manifesting synthesis of cg-N. The following two arrangements are mostly evident: (a) absorber made of CVD (diamond grown by chemical vapor deposition) diamond plate and cBN/epoxy gasket, and (b) boron absorber and Re gasket. In both cases we obtained only x-ray reflections corresponding to the cg-N structure. This means that the observed diffraction pattern does not relate to compounds of nitrogen with rhenium or boron. Reaction with carbon is also excluded because the CVD plate heater apparently does not react with nitrogen at temperatures of up to 2,500 K: diffraction from the heated polycrystalline CVD plate presents only diamond rings which have same intensity as the unheated plate. We also did not observe any Raman peaks in the range of  $200\text{--}3,500\text{ cm}^{-1}$  except of the cg-N peak at  $\approx 830\text{ cm}^{-1}$  and the vibron of a small intensity – a reminder of incomplete transformation of molecular nitrogen. Reaction with diamond anvils is also excluded for the following reason. We know that molecular nitrogen nearly completely transforms at the new phase (the molecular vibron disappeared). The thickness of the nitrogen sample in our experiments was  $\sim 5\text{ }\mu\text{m}$ . This means that diamond anvils should be etched at  $> 1\text{ }\mu\text{m}$  in depth to create a hypothetical carbonitride compound. We did not see any changes at the surface of the anvils after the experiments while submicroscopic changes can be easily seen with the interference microscope. Indeed, in rare cases occasionally we damaged the diamond surface with sharply focused laser radiation but these spots were visually easy to identify. In addition, Raman spectra from the damaged areas revealed peaks related to carbonitriles but not the cg-N peak. Finally, diamonds are warmed to less than  $100^\circ$  during laser heating, as we measured with a Pt thermometer (Pt foil touched to an anvil). Therefore, reaction of nitrogen with diamonds is unlikely.

### 2.3 Transformation from Molecular to Polymeric Nitrogen

In this section we will discuss details of transformation of molecular to polymeric nitrogen. First, we estimate a minimum pressure of the phase transformation. For that, we heated a sample of nitrogen at successively increasing pressures. At 20 GPa and 800 K and at 60 GPa and 2,500 K no changes in the Raman spectra were observed. At 82 GPa we saw no significant changes in the Raman spectra below 2,400 K. After heating at this temperature, a peak at  $2,392\text{ cm}^{-1}$  from a new molecular nitrogen phase was observed below the main vibron line of molecular nitrogen at  $2,410\text{ cm}^{-1}$ , indicating reduced bond order of the N–N bond and charge redistribution due to enhanced interaction between molecules [41]. At 95 GPa, this phase disappeared after heating to 1,500 K and only the previously known molecular phase was observed after heating up to 2,590 K. After increasing pressure to 110 GPa, the sample behaved similar to other experiments on synthesis of cg-N (as shown, for instance, in Fig. 2.3). Luminescence strongly increases at temperatures above 800 K (Fig. 2.8). This is apparently due to accumulation of defects in the crystalline lattice. After heating to higher temperature of 1,520 K luminescence decreases but nitrogen obviously remains in the molecular form – intensity of the vibron remains the same

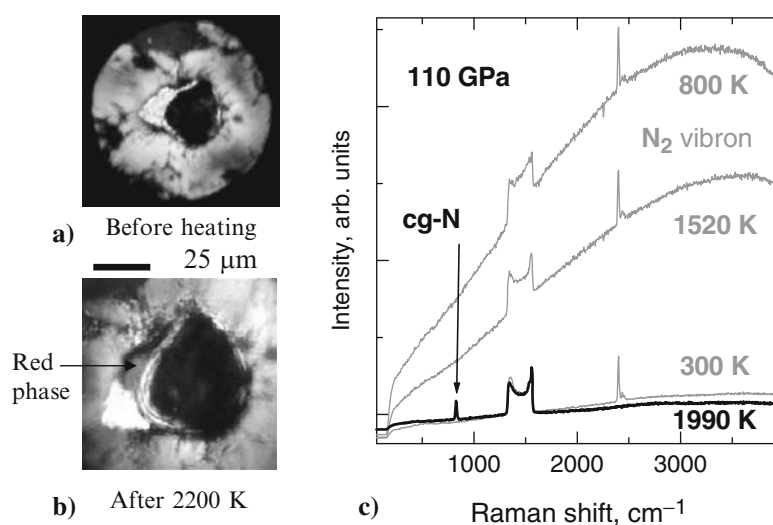


**Fig. 2.8** Laser heating of molecular nitrogen at 110 GPa. **(a)** View of the sample through diamond anvils. Nitrogen is contained in a hole in rhenium gasket where a  $1\text{ }\mu\text{m}$  thick boron plate black is placed as an absorber of heating radiation of YAG laser. Nitrogen is over the plate and seen as transparent at the left corner of the hole of the Re gasket which surrounds the sample. **(b)** After laser heating up to 1,990 K nitrogen transforms to cg-N which can be seen around the boron absorber as yellow or colorless substance. A transient red phase is at periphery of the heated area. Nitrogen remained in molecular form in the unheated corner of the sample at the left. **(c)** Raman spectra of nitrogen measured at room temperature after heating to the mentioned temperatures. In result of heating to 1,990 K vibron disappeared and a peak corresponding to cg-N phase appeared

and no other peaks appear. Drastic spontaneous transformation happens at heating to  $\sim 2,000$  K: nitrogen transforms to a nonmolecular form (the vibron disappears) and a cg-N single-bonded nitrogen forms with a characteristic Raman peak at  $820\text{ cm}^{-1}$ . During laser heating at the transformation, the temperature drops for several hundred degrees so that additional power is needed to maintain the temperature. Upon the transformation, pressure significantly drops on 5–20 GPa (depending on particular arrangement of the sample in the chamber) indicating a significant reduction of the volume of the sample. The phases of the transformation can be seen in Fig. 2.8. The cg-N looks colorless or yellow over the boron absorber and at its edge. A transient high luminescence amorphous phase is formed at the colder part of sample. It is red and is well separated from the cg-N phase. The colorless molecular nitrogen remains unchanged in the unheated part of the sample.

In many other experiments we observed that nitrogen remains in molecular form at pressures lower than 110 GPa, even being heated to 3,000 K. At higher pressures, the needed temperature is lower: for instance, at 140 GPa cg-N can be created at  $T \sim 1,400$  K.

For further clarification of transformation of molecular to polymeric nitrogen the starting structure - knowledge of the crystal structure of molecular nitrogen is required. However, it is available only below approximately 50 GPa where the diatomic solid nitrogen exhibits a rich phase diagram [59, 60]. At higher pressures of  $\sim 60$  GPa at room temperature, Raman and infrared absorption data indicate a transformation from the  $\epsilon$ -N<sub>2</sub> rhombohedral ( $R3c$ ) [61–63] to a  $\zeta$ -N<sub>2</sub> phase [60, 64, 65]. This phase persists in the molecular state up to further transformation to the non-molecular state at 150–180 GPa. The crystal structure of  $\zeta$ -N<sub>2</sub> has not yet been firmly determined. It was proposed as  $R3c$  [65, 66], but later it was found that this structure is not consistent with Raman and IR data performed at low temperatures [60, 64]. A low-symmetry (orthorhombic or monoclinic) structure with two sites for atoms was proposed [64]. In x-ray studies of nitrogen up to 65 GPa at room temperature, Jephcoat et al. [67] observed a transition at  $\sim 60$  GPa, but the signal was weak and the pressure was not high enough to separate the new phase and determine its structure. New molecular phases have also been synthesized at high pressures and temperatures (70–90 GPa and 600–1,000 K); although x-ray diffraction data are sufficient to identify them as new phases, the crystal structures have not yet been determined [48].

We performed extensive x-ray diffraction measurements of molecular nitrogen up to 170 GPa and tried to identify the structure of  $\zeta$ -N<sub>2</sub> phase. A majority of the diffraction patterns of the molecular phases were collected at the Advanced Photon Source (APS, HPCAT at Sector 16), while the cg-N-phase and some patterns of molecular nitrogen were collected at the European Synchrotron Radiation Facility (ESRF, beamlines ID-9 and ID30). In all cases, we used an x-ray beam focused down to a spot of  $\sim 5\text{ }\mu\text{m}$ , and angle dispersive diffraction techniques [19].

Diffraction patterns of nitrogen in the 60–150 GPa pressure range are shown in Fig. 2.9. At 60 GPa, several diffraction peaks of the previous  $\epsilon$ -phase widen. At 69 GPa, these peaks are split but new peaks do not appear, which suggests that the  $\epsilon$ -N<sub>2</sub>  $\rightarrow$   $\zeta$ -N<sub>2</sub> transformation is not accompanied by a large lattice distortion. Above

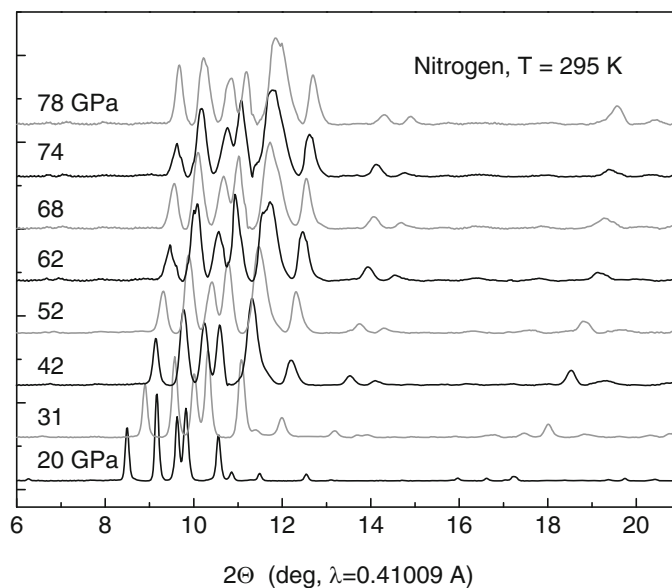


**Fig. 2.9** X-ray diffraction spectra of molecular nitrogen taken at different pressures

80 GPa, diffraction patterns demonstrate only one phase which does not change up to 150 GPa, with the exception of the appearance of an amorphous halo above 100 GPa and some redistribution of the intensity. We analyzed the diffraction pattern of the  $\zeta$ -phase obtained at 80 GPa. We tried the hexagonal indexing to verify the  $R3c$  structure. The structure was found not to be a rhombohedral structure; only hexagonal indices fit the data, verifying that the  $\zeta$ -phase does not have the  $R3c$  structure. To identify this low-symmetry structure, the best indexing was found with an orthorhombic unit cell. Three space groups:  $P222_1$ ,  $P2_12_12$ , and  $P2_12_12_1$  satisfied the diffraction spectra. The  $P222_1$  group has been selected because of its proximity to the space group  $I2_13$  (cg-N structure). However, its comparison with the cg-N structure may not be valid because a gradual martensitic transformation between these structures is unlikely. Such transition requires very high pressures, which is where the equations of state (EOS) of  $\zeta$ -N<sub>2</sub> and cg-N would intersect (Fig. 2.10). Instead, the final transition to the cg-N structure is accompanied by a drastic change in volume, approximately 22% at 110 GPa (Fig. 2.10). Note, that at this pressure, the atomic volume of the molecular phase ( $\zeta$ -N<sub>2</sub>) approaches that for cg-N at zero pressure (Fig. 2.10). The  $P222_1$  group structure is under debate [68] and further efforts on determination of apparently low-symmetry structure of  $\zeta$ -N<sub>2</sub> are needed.

Molecular-polymeric transformation in nitrogen remarkably resembles phase transformations in carbon and boron nitride in terms of compressibility and volume change (Fig. 2.10). There may also be similarities in the microscopic mechanisms of these transformations in nitrogen and carbon (and BN). Transitions between the carbon and BN phases are reconstructive diffusion-type phase transformations where

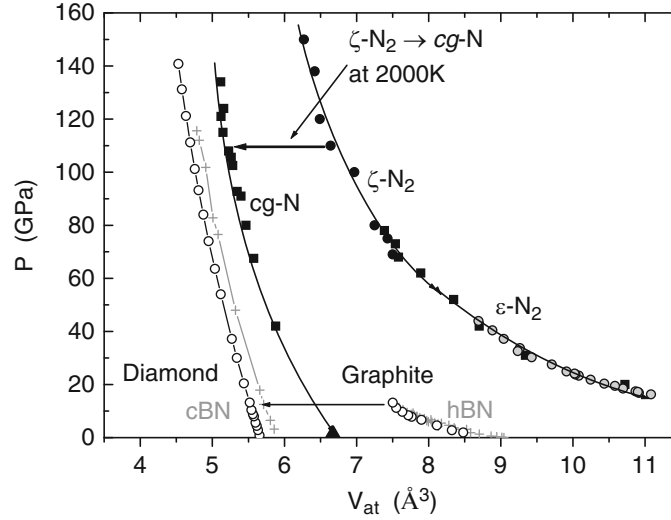


**Fig. 2.10** Pressure–volume equation of state (EOS) of nitrogen. Our experimental data for  $\epsilon$ -N<sub>2</sub> are shown with open circles. Grey circles are data from Ref. 61. At  $P > 60$  GPa  $\epsilon$ -phase transforms to  $\zeta$ -phase which remains stable at pressures up to  $P > 150$  GPa, where upon it transitions to a nonmolecular phase with an amorphous-like structure.  $\eta$ -N<sub>2</sub> can be directly transformed to the cubic gauche structure (cg-N) with laser heating above 2,000 K at  $P > 110$  GPa (Ref. [20]). The EOS of this phase has been measured with increasing pressure up to 134 GPa, and then on releasing pressure down to 42 GPa where the sample escaped the cell. Extrapolation of this EOS to zero pressure gives a volume of cg-N structure about 6.6 Å<sup>3</sup> [3] in excellent agreement with theoretical predictions of 6.67 Å<sup>3</sup> [3] (Ref. [18]). The EOSs for carbon [71, 72] graphite and diamond) and BN [73, 74] are also presented to show the proximity of these covalent bonded materials with nitrogen

growth of a new phase can be accompanied by the fragmentation of the parent crystal and the creation of a disordered amorphous layer between crystallites, as has been reported for the hBN  $\leftrightarrow$  cBN transitions [69]. Similarly, it has been proposed recently that such transformations can occur through virtual melting along interfaces in the material [70]. This general picture of fragmentation of phases and creation of amorphous material is consistent with the disordered state of the nonmolecular nitrogen.

To check, if transformation from molecular to cg-N goes through an amorphous phase, or a transient phase [41] we performed for the first time x-ray diffraction in situ with laser heating. This experiment requires a combination of two complex techniques: x-ray diffraction measurements from light elements like nitrogen, and laser heating at megabar pressures. We performed measurements at 13 ID beam line at APS (Chicago). An intensive x-ray beam of 0.3344 Å wavelength was collimated to  $\approx 5 \mu\text{m}$  spot. This beam produced a luminescence in the sample, therefore, the beam can be visualized with a sensitive CCD camera. This helped us to combine precisely the x-ray and laser-heating beams. The YAG laser beam was focused to a larger spot



than the x-ray beam to diameter of  $\approx 10\mu\text{m}$ , and therefore diffraction has been collected from nearly uniformly heated area. Temperature was determined by recording the spectrum of thermal radiation and fitting it with the Planck radiation function.

An important experimental improvement is the already mentioned toroidal shape of diamond anvil culet (Fig. 2.7). This allowed us to increase thickness of the sample to  $\approx 14\text{--}15\mu\text{m}$  (with flat anvils it is  $\approx 3\text{--}5\mu\text{m}$ ) and thus dramatically increase x-ray scattering and decrease accumulation time of a nitrogen sample to seconds.

As squeezed to pressure about 140 GPa, the nitrogen sample becomes partly dark, and no Raman signal could be detected from the dark sample, indicating the transition to the amorphous nonmolecular phase in agreement with previous studies [14, 15, 47]. However, the area in the center of the sample remained in molecular state as inferred by Raman spectra typical for molecular  $\zeta\text{-N}_2$  phase. The x-ray diffraction pattern obtained from this part of sample can also be attributed to the molecular  $\zeta$ -phase while no diffraction peaks were observed in diffraction pattern from the dark region of the amorphous sample. As the sample was heated above 1,000 K, the intensity of diffraction lines of  $\zeta$ -phase gradually decreases (Fig. 2.7) indicating the decrease of the amount of this phase. No new diffraction lines indicating the transformation to a new crystalline phase could be detected in the diffraction pattern. With temperature increase, the molecular  $\zeta$ -phase transforms to the amorphous state. At  $T \sim 1,450\text{ K}$  the diffraction lines of  $\zeta$ -phase disappears completely. This transformation to the amorphous phase is irreversible – the diffraction pattern of the sample quenched to the room temperature does not reveal reflections from  $\zeta$ -phase. This amorphous phase is nonmolecular as inferred by the absence of vibron lines in the Raman spectra of the quenched sample. In the subsequent heating of this part of the sample containing the amorphous material the well-defined diffraction pattern of newly formed cg-N appeared as the sample was heated above 1,300 K. The amount of the cg-phase was growing with further temperature increase up to a highest temperature of about 2,000 K. No changes of diffraction pattern were observed as the sample was cooled down to room temperature. The same sequence of transformations (molecular  $\rightarrow$  amorphous  $\rightarrow$  cg-nitrogen [cgN]) was reproducibly observed at continuous increases in temperature of unheated parts of the sample with laser. In this manner nearly the whole sample was entirely transformed to the cg-phase revealing a very pronounced diffraction pattern (Fig. 2.7).

Our data evidence that at high pressure–high temperatures molecular nitrogen transforms to the atomic cg-N through an amorphous state. This transformation between solid molecular and cg-nitrogen occurs with continuous increase of temperature at the same pressure; therefore, this is a solid-state transformation without melting. The amorphous state is likely a polymeric network of single-bonded and double-bonded nitrogen atoms as follows from calculations [16, 17]. An amorphous state intermediate between phases is typical for diffusion-type phase transformations. It has been clearly observed in transformations with large change of volume to such as graphite-diamond ( $\Delta V \approx 26\%$ ) [71–73] and hexagonal BN – cBN ( $\Delta V \approx 24\%$ ) transformations [73, 74]. The molecular–cg-N transitions is also diffusion-type first-order transition between very different structures with a large drop of volume ( $\Delta V \approx 22\%$ ).

### 2.3.1 Metastability of Polymeric Nitrogen and its Recovery

Another aspect of transitions with large change of lattices and volume is a large hysteresis of the phase transformation and metastability – once formed, a high-pressure phase can be recovered to ambient pressure (a well-known example is diamond). From an energetic point of view a reason of metastability is a large kinetic barrier separating high- and low-pressure phases. For carbon, the energetic barrier at zero pressure between graphite and diamond is  $\Delta E \approx 0.33 \text{ eV atom}^{-1}$  (Fig. 2.11) and  $0.38 \text{ eV pair}^{-1}$  for BN [73–75] while the energy difference between diamond and hexagonal graphite is nearly zero [73]. Therefore, diamond (which has slightly higher energy) separated by the large barrier from graphite is practically as stable as graphite.

In difference with cBN or diamond, nitrogen in polymeric state has much higher energy than in the ground state (molecular nitrogen): this difference is  $\sim 1.2\text{--}1.3 \text{ eV atom}^{-1}$ . However, to transform from cg-N to molecular nitrogen a barrier of  $\sim 0.9 \text{ eV}$  [18] should be overcome (Fig. 2.11). The activation energy  $E_A = 0.63 \text{ eV}$  is also characteristic for the amorphous polymeric nitrogen (which has a short-range with predominantly threefold coordinated atoms) as calculated in Ref. [16]. These large barriers suggest that the highly energetic cg-N and the amorphous polymeric nitrogen might be metastable even at zero pressure [18, 39]. More careful consideration includes surface. Unsaturated bonds which are intrinsic defects on the surface of cg-N crystal significantly decrease the barrier [16] down to  $\sim 0.1 \text{ eV}$  [29]. Still this is a high barrier which implies that cg-N might be stable at ambient pressure at least at low temperatures. Note, that the broken bonds at the

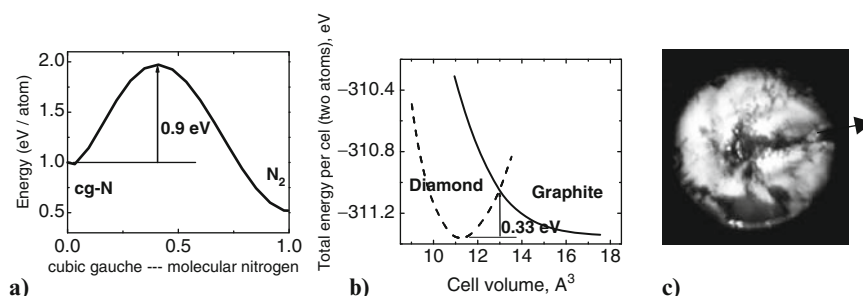


**Fig. 2.11** Energy barriers separated a metastable phases from a ground state. (a) Calculated total energy per atom as a function of the reaction coordinate for  $\text{cg} \rightarrow \beta'\text{-O}_2$  transformation, where  $\beta'\text{-O}_2$  designates a distorted two-layer variant of the  $\beta\text{-O}_2$  molecular structure. This is approximately zero pressure path, with the starting atomic volumes equal to the equilibrium values for the cg-N phase ( $6.67 \text{ \AA}^3 \text{ atom}^{-1}$ ) and the final volume the equilibrium value for  $\beta\text{-O}_2$  molecular ( $19.67 \text{ \AA}^3 \text{ atom}^{-1}$ ). The zero of energy corresponds to the diatomic  $\beta\text{-O}_2$  structure (from Ref. [18]). (b) Graphite-diamond relation. Total energy per cell (two atoms), as functions of the cell volume for the hydrostatic pressure path. In (a) the solid curve is for the graphite and the dashed curve is for the diamond (from Ref. [73]). (c) A typical example of the rhenium gasket broken by the cg-N sample escaped from the cell at 70 GPa in direction shown by the arrow

surface which are the nuclei of instability can be saturated by hydrogen atoms [29]. This is similar as in the case of amorphous polymeric nitrogen [16].

The above estimation suggest possibility of recovering of polymeric nitrogen. However, this turned out to be a difficult experimental problem: typically the sample escapes from the diamond anvil cell at pressures of 70–100 GPa by rupturing the gasket. This is a typical occurrence, and obviously this is due to the inherent weakening of the gasket at decreasing pressure [56]: at releasing, load edges of diamond culet elastically recover and do not support the plastically deformed thin gasket anymore. A novel technique must be developed for repetitive recovery of the sample at ambient pressure. Nevertheless, after a number of efforts amorphous nonmolecular nitrogen once has been recovered to ambient pressure at temperatures below 100 K [14]. Cg-N has not been recovered yet – it also escapes at the same pressures at our numerous attempts with different configurations of the gasket and the anvils. At present pressure down to 42 GPa has been achieved occasionally due to a sudden drop of pressure from 115 GPa because of failure of one of the anvils. The sample of cg-N nevertheless survived but partly transformed to molecular nitrogen. At this pressure and 300 K it was apparently unstable – it had transformed to molecular nitrogen (cg-N Raman peak disappeared) under approximately 40 min of focused laser radiation of wavelength of 488 nm and power of  $W = 10$  mW. This behavior is similar to nonmolecular amorphous nitrogen which transformed back to molecular form at  $P < 50$  GPa at 300 K [14]. This indicates that most likely both forms of non-molecular nitrogen are polymeric nitrogen in disordered or single-crystalline forms. This also means that cg-N will be likely recovered to ambient pressure similar to the amorphous nitrogen.

### 2.3.2 Perspectives of Synthesis of New Forms Polymeric Nitrogen

Starting from prediction of polymeric nitrogen [12, 18] theoretical calculations give insight to its properties and stimulated experiment. Recent calculations become more and more precise and can predict amazingly well structures of high-pressure phases. In our experience, we found nearly exact prediction of high-pressure phases in silane [76, 77], see also Ref. [23]. In this respect theoretical exploration of the new polymeric nitrogen structure [16, 23–31, 33, 37, 38, 42–44] is very promising and can guide direction of experimental search. These calculations agree that cg-N structure is the most stable. Besides, many other structures were found which are close in energy to cg-N, for instance, another three-dimensional polymeric structure related to cubic gauche (Fig. 2.7) and less stable by only  $49 \text{ meV atom}^{-1}$  [23].

Systematic search of new metastable allotropes of nitrogen has been done by Zahariev et al. [28]. They considered Peierls-like distortions of a reference structure which was taken simple cubic structure (SC) which is to be the natural high-pressure reference structure for group 15 elements. They found many structures with total energy close to cg-N, which clearly has the lowest enthalpy. Two structures were discovered to be mechanically stable at zero pressure. Notably, all the previously considered simple single-bonded phases of polymeric nitrogen (BP, A7, and LB)

with the exception of cg-N, were found to be mechanically unstable at all pressures considered.

There is a number of works, predicting new nonmolecular phases compatible to cg-N in the low-pressure region. *Chaired web* (CW) structure was found which is thermodynamically more stable than the cubic gauche (cg-N) phase at the ambient pressure: the enthalpy favors CW over CG by approximately 20 meV [31]. The temperature-dependent free-energy and zero-point energy corrections favor cg-N over CW by 54 meV. With the rise in temperature there is a crossover of the two free-energy dependences around 200 K. At ambient temperature the new CW phase is thermodynamically more stable than the cg-N. Metastability of the CW phase was demonstrated by both phonon calculations, and first-principles molecular dynamics simulations. The CW phase is an insulator at low pressure with a calculated band gap of  $\sim 5$  eV.

Alemay and Martins [37] also predicted a phase which has lower enthalpy than cg-N at  $P < 15$  GPa. It has a zigzag chainlike arrangement is thus partially polymeric and each atom has a coordination number of two. This phase is metastable at zero pressure and is metallic. Mattson et al. [25] found a very similar and also metallic chain structure but with the different packing which leads to a significantly lower energy ( $\sim 0.18$  eV/atom<sup>-1</sup>) [25] making it very close in energy (but slightly higher) to cg-N. A new structure with the zigzag chains in the new phase connected by two atoms with double bonds has been proposed in Ref. [44], but it has higher energy than other chain phases.

Stability of cg-N in the limit of high pressures was studied by Alemay and Martins [37]. They found that at  $P > 200$  GPa BP, an orthorhombic distortion of sc is more stable than CG.

Experimentally all these predicted nonmolecular phases were not yet confirmed.

Theoretical calculations gave further insight of unique properties of cg-N. This is a wide energy gap dielectric: the band gap is 4.13 eV at zero pressure and 3.89 eV at 240 GPa [27], and 5.2 eV at 150 GPa in Ref. [38]. The generalized gradient approximation (GGA) calculation of the band gap at 240 GPa is in good agreement with previous work [37] while Monte Carlo calculations [32] give band gap 8.1 eV. Chen et al. [42] found the unique constant-gap behavior ( $E_g = 4.2$  eV under pressures 40 and 130 GPa, and it decreases at lower and higher pressures. The  $E_g \sim 4$  eV at megabar pressures well correlates with our observations of the colorless transparent phase. Further detailed calculations of compressibility, lattice dynamics [24], dielectric constants  $\epsilon^\infty = 4.44$ ,  $\epsilon^0 = 4.81$  at  $P_0$  of cg-N and their pressure dependence have been done in Ref. [41].

Chen et al. [42] raised attention to an interesting possibility that cg-N can be also a superhard material. The distance between nitrogen atoms in the cg-N at ambient pressure is 1.466 Å [19] – significantly shorter than that for diamond (1.54 Å). The high strength of cg-N is also indicated by its high bulk modulus: 260–340 GPa [18, 19, 21, 27, 38, 44, 50]. On the other hand, strength of cg-N could be weaker in comparison with diamond because there are only three bonds for each atom for nitrogen instead of four bonds for diamond. Chen et al. [42] calculated the hardness of cg-N as  $\approx 83$  GPa which is less than diamond (100–130 GPa) but higher than other known superhard materials: (c – BC<sub>2</sub>N (76 GPa) and cBN (63 GPa)).

## 2.4 Conclusions

It is shown here that pure nitrogen can exist in polymeric forms where atoms connect each other by single covalent bonds. At room or lower temperatures nitrogen transforms to an amorphous polymeric form at 150–200 GPa. Under laser heating at  $T \sim 2,000$  K and  $P > 110$  GPa nitrogen has been synthesized in a single-bonded crystalline form. It has unusual cubic gauche structure (cg-N) with space group  $I2_13$ . In the cg-N structure all-nitrogen atoms are threefold coordinated and bond-lengths are the same for all pairs of bonded atoms. The experimentally determined structure is in perfect agreement with the theoretical prediction. Polymeric nitrogen can be metastable at ambient pressure as has been confirmed experimentally for the amorphous phase. The metastable polymeric nitrogen is predicted to be the most powerful high-density energy, because of a uniquely large difference in energy between single-bonded and triple-bonded atoms. In particular, it was calculated that polymeric nitrogen can produce detonation pressure ten times higher than that for HMX. Interestingly, cg-N is also predicted to be a superhard material second after diamond.

It is also shown here that high nitrogen materials can be prepared at lower pressure utilizing starting materials other than pure nitrogen. The challenge remains the recovery of such new high-energy density high-nitrogen or pure-nitrogen materials down at ambient pressures and temperatures.

## References

1. Huheey, J. E., Keiter, E. A. & Keiter, R. L. *Inorganic Chemistry: Principles of Structure and Reactivity* (Harper Collins, New York, 1993).
2. Christe, K. O. Recent Advances in the Chemistry of  $N_5^+$ ,  $N_5^-$  and High-Oxygen Compounds. *Propel, Explosiv. Pyrotech.* **32**, 194–204 (2007).
3. Samartzis, P. C. & Wodtke, A. M. All-nitrogen chemistry: how far are we from  $N_{60}$ ? *Int. Rev. Phys. Chem.* **25** 527–552 (2006).
4. Rice, B. M., Byrd, E. F. C. & Mattson, W. D. Computational aspects of nitrogen-rich HEM. *High Ener Density Mater. Struct. Bond.* **125**, 153–194 (2007).
5. Barlett, R. J. Exploding the mysteries of nitrogen. *Chem. Indus.* 140–143 (2000).
6. Cacase, F., Petris, G. d. & Troiani, A. Experimental detection of tetranitrogen. *Science* **295**, 480–481 (2002).
7. Curtius, T. *Berichte. Deutsch. Chem. Gesellschaft* **23**, 3023–3033 (1890).
8. Christe, K. O., Wilson, W. W., Sheehy, J. A. & Boatz, J. A.  $N_5^+$ : A novel homolepic polynitrogen ion as a high energy density material. *Angew. Chem. Int. Ed.* **38**, 2002–2009 (1999).
9. Klapotke, T. M. in *High Energy Density Materials* (ed. Klapotke, T. M.), pp. 85–121 (Springer, Heidelberg, 2007).
10. Knapp, C. & Passmore, J. On the Way to “Solid Nitrogen” at Normal Temperature and Pressure? Binary Azides of Heavier Group 15 and 16 elements. *Angew. Chem. Int. Ed.* **43**, 2–4 (2004).
11. Glukhovtsev, M. N., Jiao, H. & Schleyer, P. v. R. Besides  $N_2$ , what is the most stable molecule composed only of nitrogen atoms? *Inorg. Chem.* **35**, 7124–7133 (1996).
12. McMahan, A. K. & LeSar, R. Pressure dissociation of solid nitrogen under 1 Mbar. *Phys. Rev. Lett.* **54**, 1929–1932 (1985).

13. Martin, R. M. & Needs, R. Theoretical study of the molecular-to-nonmolecular transformation of nitrogen at high pressures. *Phys. Rev. B* **34**, 5082–5092 (1986).
14. Eremets, M. I., Hemley, R. J., Mao, H. K. & Gregoryanz, E. Semiconducting non-molecular nitrogen up to 240 GPa and its low pressure stability. *Nature* **411**, 170–174 (2001).
15. Goncharov, A. F., Gregoryanz, E., Mao, H. K., Liu, Z. & Hemley, R. J. Optical evidence for nonmolecular phase of nitrogen above 150 GPa. *Phys. Rev. Lett.* **85**, 1262–65 (2000).
16. Nordlund, K., Krashennnikov, A., Juslin, N., Nord, J. & Albe, K. Structure and stability of non-molecular nitrogen at ambient pressure. *Europ. Lett.* **65**, 400–406 (2004).
17. Mattson, W. D. PhD thesis (University of Illinois at Urbana-Champaign, 2003).
18. Mailhot, C., Yang, L. H. & McMahan, A. K. Polymeric nitrogen. *Phys. Rev. B* **46**, 14419–14435 (1992).
19. Eremets, M. I., Gavriluk, A. G., Trojan, I. A., Dzivenko, D. A. & Boehler, R. Single-bonded cubic form of nitrogen. *Nature Mater.* **3**, 558–563 (2004).
20. Gregoryanz, E. et al. High P-T transformations of nitrogen to 170 GPa. *J. Chem. Phys.* **126**, 184505 (2007).
21. Lipp, M. J. et al. Transformation of molecular nitrogen to nonmolecular phases at megabar pressures by direct laser heating. *Phys. Rev. B* **76**, 014113 (2007).
22. Trojan, I. A., Eremets, M. I., Medvedev, S. A., Gavriluk, A. G. & Prakapenka, V. B. Transformation of molecular to polymeric nitrogen at high pressures and temperatures. In situ X-ray diffraction studies. *Appl. Phys. Lett.*, to be published (2008).
23. Oganov, A. R. & Glass, C. W. Crystal structure prediction using ab initio evolutionary techniques: Principles and applications. *J. Chem. Phys.* **124**, 244704 (2006).
24. Caracas, R. Raman spectra and lattice dynamics of cubic gauche nitrogen. *J. Chem. Phys.* **127**, 144510 (2007).
25. Mattson, W. D., Sanchez-Portal, D., Chiesa, S. & Martin, R. M. Prediction of new phases of nitrogen at high pressure from first-principles simulations. *Phys. Rev. Lett.* **93**, 125501–125504 (2004).
26. Zahariev, F., Hu, A., Hooper, J., Zhang, F. & Woo, T. Layered single-bonded nonmolecular phase of nitrogen from first-principles simulation. *Phys. Rev. B* **72**, 214108 (2005).
27. Yu, H. L. et al. First-principles calculations of the single-bonded cubic phase of nitrogen. *Phys. Rev. B* **73**, 012101 (2006).
28. Zahariev, F., Dudiy, S. V., Hooper, J., Zhang, F. & Woo, T. K. Systematic method to new phases of polymeric nitrogen under high-pressure. *Phys. Rev. Lett.* **97**, 155503–1555034 (2006).
29. Zhang, T., Zhang, S., Chen, Q. & Peng, L.-M. Metastability of single-bonded cubic-gauche structure of N under ambient pressure. *Phys. Rev. B* **73**, 094105–094107 (2006).
30. Uddin, J., Barone, V. N. & Scuseria, G. E. Energy storage capacity of polymeric nitrogen. *Molecul. Phys.* **104**, 745–749 (2006).
31. Zahariev, F., Hooper, J., Alavi, S., Zhang, F. & Woo, T. K. Low-pressure metastable phase of single-bonded polymeric nitrogen from a helical structure motif and first-principles calculations. *Phys. Rev. B* **75**, 140101 (2007).
32. Mitas, L. & Martin, R. M. Quantum Monte Carlo of nitrogen: atom, dimer, atomic, and molecular solids. *Phys. Rev. Lett.* **72**, 2438–2441 (1994).
33. Lewis, S. P. & Cohen, M. L. High-pressure atomic phases of solid nitrogen. *Phys. Rev. B* **46**, 11117–11120 (1992).
34. Eremets, M. I. et al. Polymerization of nitrogen in sodium azide. *J. Chem. Phys.* **120**, 10618–10618 (2004).
35. Peiris, S. M. & Russell, T. P. Photolysis of Compressed Sodium Azide ( $\text{NaN}_3$ ) as a synthetic pathway to nitrogen materials. *J. Phys. Chem. A* **107**, 944–947 (2003).
36. Hemley, R. J. Effects of high pressure on molecules. *Annu. Rev. Phys. Chem.* **51**, 763–800 (2000).
37. Alemany, M. M. G. & Martins, J. L. Density-functional study of nonmolecular phases of nitrogen: metastable phase at low pressure. *Phys. Rev. B* **024110** **68**, 024110 (2003).
38. Zhao, J. First-principles study of atomic nitrogen solid with cubic gauche structure. *Phys. Lett. A* **360**, 645–648 (2007).



39. Barbee, T. W. & III. Metastability of atomic phases of nitrogen. *Phys. Rev. B* **48**, 9327–9330 (1993).
40. Yakub, E. S. Diatomic fluids at high pressures and temperatures: a non-empirical approach. *Physica B* **265**, 31–38 (1999).
41. Caracas, R. & Hemley, R. J. New structures of dense nitrogen: pathways to the polymeric phase. *Chem. Phys. Lett.* **442**, 65–70 (2007).
42. Chen, X. Q., Fu, C. L. & Podloucky, R. Superhard Dense Nitrogen. *Phys. Rev. B* **77**, 064103 (2008).
43. Ross, M. & Rogers, F. Polymerization, shock cooling, and the high-pressure phase diagram of nitrogen. *Phys. Rev. B* **74**, 024103 (2006).
44. Wang, X. L. et al. Prediction of a new layered phase of nitrogen from first-principles simulations. *J. Phys.: Condens. Matter*, **19**, 425226–425229 (2007).
45. Reichlin, R., Schiferl, D., Martin, S., Vanderborgh, C. & Mills, R. L. Optical studies of nitrogen to 130 GPa. *Phys. Rev. Lett.* **55**, 1464–1467 (1985).
46. Bell, P. M., Mao, H. K. & Hemley, R. J. Observations of solid H<sub>2</sub>, D<sub>2</sub>, N<sub>2</sub> at pressures around 1.5 megabar at 25°C. *Physica B* **139–140**, 16–20 (1986).
47. Gregoryanz, E., Goncharov, A. F., Hemley, R. J. & Mao, H. K. High-pressure amorphous nitrogen. *Phys. Rev. B* **64**, 052103 (2001).
48. Gregoryanz, E. et al. Raman, infrared, and x-ray evidence for new phases of nitrogen at high pressures and temperatures. *Phys. Rev. B* **66**, 224108–5 (2002).
49. Eremets, M. I., Struzhkin, V. V., Mao, H. K. & Hemley, R. J. Superconductivity in boron. *Science* **293**, 272–274 (2001).
50. Eremets, M. I., Gavriluk, A. G., Trojan, I. A., Dzivenko, D. A. & Boehler, R. in *ESRF High-lights 2004* (ed. Admans, G.), pp. 37–38 (Imprimerie du Pont de Claix, Grenoble, 2005).
51. Sanz, D. N., Loubeyre, P. & Mezouar, M. Equation of state and pressure induced amorphization of  $\beta$ -boron from X-ray measurements up to 100 GPa. *Phys. Rev. Lett.* **89**, 245501 (2002).
52. Yoo, C. S., Akella, J., Cynn, H. & Nicol, M. Direct elementary reactions of boron and nitrogen at high pressures and temperatures. *Phys. Rev. B* **56**, 140–146 (1997).
53. Boehler, R., Bagen, N. v. & Chopelas, A. Melting, thermal expansion, and phase transitions of iron at high pressures. *J. Geophys. Res. B* **95**, 21731–21736 (1990).
54. Mao, H. K., Xu, J. & Bell, P. M. Calibration of the ruby pressure gauge to 800 kbar under quasihydrostatic conditions. *J. Geophys. Res.* **91**, 4673–4676 (1986).
55. Eremets, M. I. Megabar high-pressure cells for Raman measurements. *J. Raman Spectr.* **34**, 515–518 (2003).
56. Eremets, M. I. *High Pressures Experimental Methods* (Oxford University Press, Oxford, 1996).
57. Knittle, E., Wentzcovitch, R. M., Jeanloz, R. & Cohen, M. L. Experimental and theoretical equation of state of cubic boron nitride. *Nature* **337**, 349–352 (1989).
58. Eremets, M. I., Gavriluk, A. G. & Trojan, I. A. Single-crystalline polymeric nitrogen. *Appl. Phys. Lett.* **90**, 171904 (2007).
59. Manzhelii, V. G. & Freiman, Y. A. (eds.) *Physics of Cryocrystals* (American Institute of Physics, College Park, MD, 1997).
60. Bini, R., Ulivi, L., Kreutz, J. & Jodl, H. J. High-pressure phases of solid nitrogen by Raman and infrared spectroscopy. *J. Chem. Phys.* **112**, 8522–8529 (2000).
61. Mills, R. L., Olinger, B. & Cromer, D. T. Structures and phase diagrams of N<sub>2</sub> and CO to 13 GPa by x-ray diffraction. *J. Chem. Phys.* **84**, 2837–2845 (1986).
62. Olijnyk, H. High pressure x-ray diffraction studies on solid N<sub>2</sub> up to 43.9 GPa. *J. Chem. Phys.* **93**, 8968–8972 (1990).
63. Hanfland, M., Lorenzen, M., Wassilew-Reul, C. & Zontone, F. Structures of molecular nitrogen at high pressure. *Rev. High Pressure Sci. Technol.* **7**, 787–789 (1998).
64. Goncharov, A. F., Gregoryanz, E., Mao, H.-K. & Hemley, R. J. Vibrational dynamics of solid molecular nitrogen to megabar pressures. *Low Temper. Phys.* **27**, 866–869 (2001).
65. Schiferl, D., Buchsbaum, S. & Mills, R. L. Phase transitions in nitrogen observed by Raman spectroscopy from 0.4 to 27.4 GPa at 15 K. *J. Phys. Chem.* **89**, 2324–2330 (1985).



66. LeSar, R. Improved electron-gas model calculations of solid N<sub>2</sub> to 10 GPa. *J. Chem. Phys.* **81**, 5104–5108 (1984).
67. Jephcoat, A. P., Hemley, R. J., Mao, H. K. & Cox, D. E. Pressure-induced structural transitions in solid nitrogen. *Bull. Am. Phys. Soc.* **33**, 522 (1988).
68. Gregoryanz, E. et al. On the epsilon-zeta transition of nitrogen. *J. Chem. Phys.* **124**, 116102 (2006).
69. M. I. Eremets et al. Disordered state in first-order phase transitions: Hexagonal-to-cubic and cubic-to-hexagonal transitions in boron nitride. *Phys. Rev. B* **57**, 5655–5660 (1998).
70. Levitas, V. I., Henson, B. F., Smilowitz, L. B. & Asay, B. W. Solid-solid phase transformation via virtual melting significantly below the melting temperature. *Phys. Rev. Lett.* **92**, 235702-1-4 (2004).
71. Hanfland, M., Beister, H. & Syassen, K. Graphite under pressure: equation of state and first-order Raman modes. *Phys. Rev. B* **39**, 12598–12603 (1989).
72. Occelli, F., Loubeyre, P. & LeToullec, R. Properties of diamond under hydrostatic pressures up to 140 GPa. *Nature Materials* **2**, 151–154 (2003).
73. Furthmüller, J., Hafner, J. & Kresse, G. Ab initio calculation of the structural and electronic properties of carbon and boron nitride using ultrasoft pseudopotentials. *Phys. Rev. B* **50**, 15606–15622 (1994).
74. Albe, K. Theoretical study of boron nitride modifications at hydrostatic pressures. *Phys. Rev. B* **55**, 6203–6210 (1997).
75. Fahy, S., Louie, S. G. & Cohen, M. L. Pseudopotential total-energy study of the transition from rhombohedral graphite to diamond. *Phys. Rev. B* **34**, 1191–1199 (1986).
76. Eremets, M. I., Trojan, I. A., Medvedev, S. A., Tse, J. S. & Yao, Y. Superconductivity in hydrogen dominant materials: silane. *Science* **319**, 1506–1509 (2008).
77. Pickard, C. J. & Needs, R. J. High-pressure phases of silane. *Phys. Rev. Lett.* **97**, 045504 (2006).

<http://www.springer.com/978-3-540-68146-5>

Static Compression of Energetic Materials

Peiris, S.M.; Piermarini, G.J. (Eds.)

2008, XII, 330 p., Hardcover

ISBN: 978-3-540-68146-5